JACS
JOURNAL OF THE AMERICAN CHEMICAL SOCIETY
Communication
pubs.acs.org/JACS

Interplay of Tunneling, Two-State Reactivity, and Bell–Evans–Polanyi Effects in C–H Activation by Nonheme Fe(IV)O Oxidants

Debasish Mandal and Sason Shaik*

Institute of Chemistry and the Lise Meitner-Minerva Center for Computational Quantum Chemistry, The Hebrew University of Jerusalem, 91904 Jerusalem, Israel

Supporting Information

ABSTRACT: The study of C–H bond activation reactions by nonheme $Fe^{IV}O$ species with nine hydrocarbons shows that the kinetic isotope effect (KIE) involves strong tunneling and is a signature of the reactive spin states. Theory reproduces the observed spike-like appearance of plots of KIE_{exp} against the C–H bond dissociation energy, and its origins are discussed. The experimentally observed Bell–Evans–Polanyi correlations, in the presence of strong tunneling, are reproduced, and the pattern is rationalized.

Synthetic iron(IV)–oxo complexes are becoming growingly important in the chemistry of C–H bond activation.[1] The ability to characterize and comprehend the reactivity patterns of these bond-activation reactions is highly challenging due to the interplay of several reactivity factors which play a role. Among these factors are the spin states of the metal ions, which lead to two-state reactivity (TSR),[2] the bond dissociation energies (BDEs) of the C–H bonds undergoing activation and the forming FeO–H bonds, which together reflect the Bell–Evans–Polanyi (BEP) principle,[3] the radical character of the oxo ligand,[4] the reactants' distortion energies,[4a] the nature of the supporting and axial ligands of the iron(IV)–oxo,[5] and quantum mechanical tunneling (QMT).[6,7] All these factors seem to play their role. But how do these factors combine to yield a coherent picture? Here we address the question by demonstrating the interplay of the TSR, BEP principle, and QMT factors in shaping the reactivity patterns of two $Fe^{IV}O$ complexes reacting with a series of hydrocarbons, shown in Figure 1a,b.[8−10] As will emerge, QMT is state selective and is a kinetic probe of the reactive spin state.

The two iron(IV)–oxo complexes, $[Fe^{IV}O(N4Py)]^{2+}$ (**1**) and $[Fe^{IV}O(Bn\text{-}TPEN)]^{2+}$ (**2**), and the hydrocarbons in Figure 1 exhibit large deuterium kinetic isotope effects (KIE), reaching ~60[7−10] at high temperatures (313 K), and apparently involve significant QMT.[11] Additionally, **1** and **2** possess a triplet (S = 1) ground state and a low-lying quintet (S = 2) excited state, which computationally switch their energy order at the transition state (TS) and hence preferring TSR.[4a,6−10,12] On top of that, the two series exhibit a BEP-like correlation, with rates increasing with a decrease of the BDE(C–H) values.[8−10,13] Which one of these spin states is responsible for the observed tunneling, and the apparent BEP correlation? If tunneling involves passage "under the barrier", sometimes by as much as 4 kcal mol^{-1},[11] why do the series exhibit BEP correlations at all? To the best of our knowledge, this web of fundamental questions has not been addressed before, and the elucidation of the observed reactivity patterns is timely.

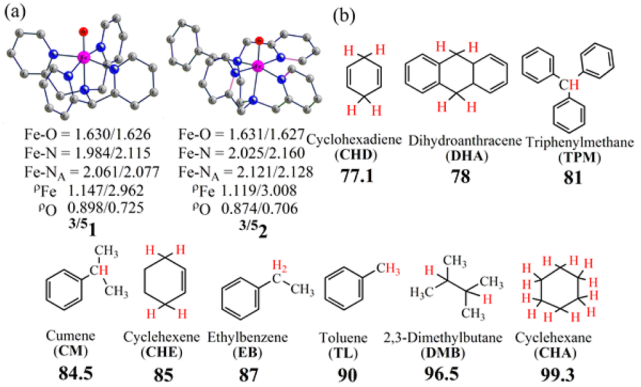

Figure 1. (a) Optimized structures of $[Fe^{IV}O(N4Py)]$ (**1**, left) and $[Fe^{IV}O(Bn\text{-}TPEN)]$ (**2**, right), used in this study with selected geometrical parameters (given in Å) and spin densities (ρ) on Fe and O. Hydrogen atoms and counterions are suppressed for clarity. N4Py = *N*,*N*-bis(2-pyridylmethyl)-*N*-bis(2-pyridyl)methylamine, Bn-TPEN = *N*-benzyl-*N*,*N*′,*N*′-tris(2-pyridylmethyl)-1,2-diaminoethane. (b) Investigated substrates and their experimental BDE(C–H) values (in bold, in kcal mol^{-1}). Equivalent H atoms are shown in red color.

As such, the series in Figure 1 are very suitable for dealing with this fundamental problem. This is done by using theoretical tools.[14] Technical details are provided in the Supporting Information (SI) document. In brief, we use UB3LYP/Def2-TZVPP//LACVP*(Fe)/6-31G*(rest)[14a,b] with solvation (SMD)[14c] and dispersion corrections (GD3BJ)[14d] implemented in Gaussian 09.[14b] Tunneling correction was calculated using an Eckart barrier,[6,14e] and the tunneling-corrected transmission coefficients were used to calculate the tunneling corrections of the barriers and KIE values.[6] As shall be demonstrated, the observed KIE is a probe of the reactive spin state of the iron-oxo reagent.[4a,6,7,15] Meanwhile, the energetic effect of tunneling will be shown to preserve the BEP effect and cause reactivity to be gauged by BDE(C–H).

Dealing with TSR requires knowledge of the spin-inversion probabilities, which are not easily accessible.[6,7,15,16] As has been shown, however,[4a,6] KIE(H/D), which is very sensitive to TS structure, can serve as a mechanistic probe of the reactive spin state. Recently,[7] a multidimensional tunneling investigation has

Received: November 21, 2015
Published: January 29, 2016

DOI: 10.1021/jacs.5b12077
J. Am. Chem. Soc. 2016, 138, 2094–2097

been carried out for the C−H activation reaction of cyclohexene (**CHE**, Figure 1b) by **1** and **2**. The computed KIE for **CHE** vs $[D]_{10}$-**CHE**, with inclusion of multidimensional tunneling, identified $S = 1$ as the primary state that participates in the C−H bond activation.[7] For the same reactions of **1** and **2** with **CHE**, we used here the simpler[6] one-dimensional Eckart calculations[14e] and got KIE values of 69 and 72, respectively, which match the 55 and 66 values computed using the multidimensional calculations. The corresponding KIE values on the $S = 2$ states are <10 in both reactions (see SI). Thus, as before,[4a,6,7,15] here too KIE serves as a kinetic signature of the reactive spin states.

As our study involves 18 reactions which possess $S = 1$ and 2 pathways, we have a total of 36 reactions, of systems which involve 100 atoms or so. As such, usage of the demanding multidimensional model is impractical for us, and instead we employ the Eckart tunneling model, which was found before[4a,6] and here to lead to KIE values in good agreement with experiment and with the multidimensional model.

To confirm the identity of the reactive spin state for other reactions in Figure 1, we show in Figure 2a,b the Eckart-based KIEs and experimentally measured ones.

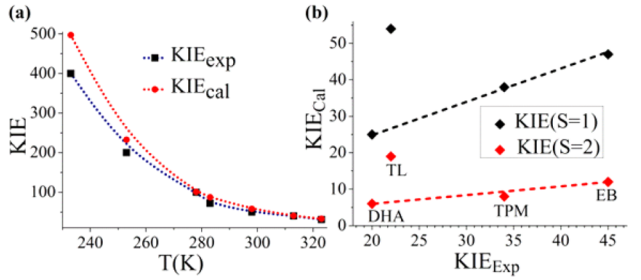

Figure 2. (a) Experimental and calculated ($S = 1$) KIEs vs temperature for the reaction between **2** with **EB** and $[D_{10}]$-**EB**. (b) Eckart-based calculated KIE($S = 1$) values vs experimentally measured ones for **1** reacting with a no of substrates (see Figure 1). Note that for **TL**, the KIE($S = 2$) value (red diamond) matches the experimental datum better than the $S = 1$ value.

Figure 2a shows plots of experimental KIE_{exp} and calculated $KIE_{cal}(S = 1)$ values vs temperatures (T), for the reaction of **2** with **EB** (see Figure 1b). In agreement with experimental findings (KIE_{exp}), the red curve of KIE_{cal} reveals a nonclassical temperature dependence. Furthermore, the red and black curves merge at high temperatures (>273 K), thus indicating a good agreement between theory and experiment. At $T < 273$ K, the KIE_{exp} curve was extrapolated from the high-temperature plot.[10] Hence, the deviation in the low-temperature range may either be due to drawbacks of Eckart-based tunneling at low-temperature or to the extrapolation procedure.[10] But the low-temperature range is anyway of no concern here.

Figure 2b further shows the reasonable correlation between KIE_{cal} values and available KIE_{exp} data. The calculated black diamond points correspond to $S = 1$, with the exception of **1** + **TL**, where the $S = 2$ KIE datum (19.2, in the red diamond) matches the experimental datum ($KIE_{exp} = 22(2)$). Thus, Figure 2 shows that the use of Eckart-tunneling is sufficiently reliable; it captures KIE magnitudes and temperature dependence and leads to clear identification of the primary reactive spin state, as generally the $S = 1$ spin state, but $S = 2$ for **1** + **TL**. Similarly, for **2**, $S = 1$ is generally identified as the reactive spin state for all substrates, with the exception of **CHA** for which the $S = 2$ value matches better the experimental datum (KIE = 7 ± 2).

The second order rates of **1** and **2** were found to exhibit good linear correlation with the hydrocarbons' BDE(C−H) values.[8,9,13] So, the reactions of **1** and **2** definitely exhibit a BEP trends and seem to be controlled by the reaction thermodynamics. However, since QMT allows passage below the barrier by variable increments,[6,7,11] it is not obvious why a BEP correlation should hold at all.

Figure 3a shows a plot of the calculated effective free energy barrier, ($\Delta G^{\ddagger}_{eff\text{-}cal}$), vs the experimental $\Delta G^{\ddagger}_{exp}$ data. The effective

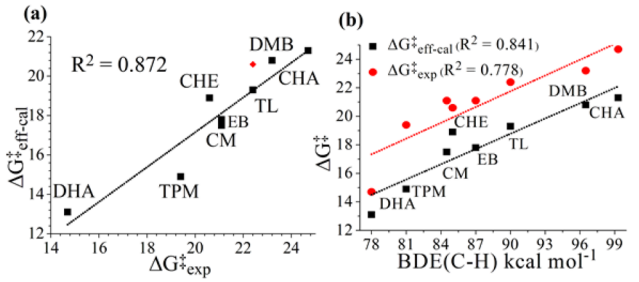

Figure 3. (a) A plot of the calculated $S = 1$ effective free energy barriers that include tunneling correction, ($\Delta G^{\ddagger}_{eff\text{-}cal}$), against the experimental data ($\Delta G^{\ddagger}_{exp}$) for **1** + the hydrocarbons in Figure 1b. For **1** + **TL** we have shown also the calculated $S = 2$ datum, as a red diamond. (b) Experimental and calculated (tunneling corrected) free energy of activation (298 K) vs BDE(C−H) values (in kcal mol^{-1}) for the reaction between **1** with all the hydrocarbons.

barriers correspond to the computed semi classical free energy barriers less the energy reduction by tunneling (see SI eq 1).[6,7] The correlation in Figure 3a is reasonable.

Figure 3b shows that both computed and experimental free energy barriers exhibit a BEP-type correlation vs the BDE(C−H). The corresponding plots for **2** are depicted in Figures S3 and S7 in the SI, showing that the barriers for **2** are lower than those for **1**, as found experimentally.[8] As such, Figure 3 shows that the experimentally observed reactivity trend is reproduced by the calculations. But how so if tunneling is involved? Indeed, despite the BEP-like correlation, tunneling is highly significant, as can be deduced from eq 1:

$$\%\ \text{tunneling} = 100[(\kappa_{Eckart} - 1)/\kappa_{Eckart}] \quad (1)$$

where κ_{Eckart} is the transmission coefficient in the Eyring equation with Eckart-tunneling included. Thus, the numerator of eq 1 is the difference between a reaction with tunneling and one having a transmission coefficient of unity, $\kappa = 1$, and devoid of tunneling. As such, the ratio $[\kappa_{Eckart} - 1)/\kappa_{Eckart}] \times 100$ gives the efficiency of tunneling. Using the computed κ values at room temperature (298 K), one gets that >95% of the reaction is carried out via tunneling, for all the reactions studied (see Table S7 in the SI). So, tunneling has a huge impact on the C−H bond activation catalyzed by the $Fe^{IV}O$ complexes, but the QMT effect seems to somehow blend into a BEP effect. How does this happen? Our calculations show that despite the dominant tunneling, its reduction of the barrier clusters around mean values with modest scatters, 3.12 ± 0.35 and 3.08 ± 0.40 kcal mol^{-1} for **1** and **2**, respectively, thus hardly affecting the apparent and anyway imperfect BEP correlation.

Let us try to comprehend the manner by which the KIEs in the target series of Figure 1 depend on the BDE(C−H) of the hydrocarbon. These features are illustrated in the four panels of

DOI: 10.1021/jacs.5b12077
J. Am. Chem. Soc. 2016, 138, 2094−2097

Figure 4. Thus, Klinker et al.[9,10] determined experimentally the KIEs for the reactions of **1** and **2** with hydrocarbons having a

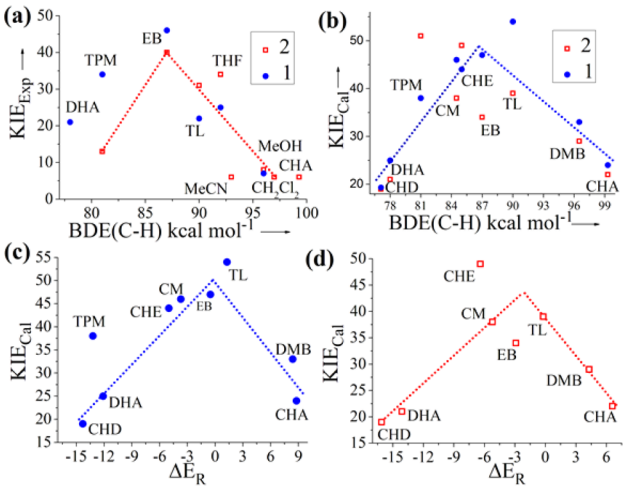

Figure 4. Plot of KIE (313 K) vs BDE(C−H) for the reaction of **1** (blue) and **2** (red): (a) experimental data[9,10] and (b) theoretical $S = 1$ data. (c and d) Theoretical $S = 1$ KIEs (313 K) vs calculated reaction energies (ΔE_R) for reactions of (c) **1** and (d) **2** (TPM, $KIE_{cal} = 51$, is off scale).

range of BDE(C−H) values and found a rough spike-type behavior of the KIE. These data are depicted in Figure 4a. It is seen that the KIE_{exp} is small for lower BDE(C−H) values and increases to a maximum values at BDE(C−H) between 85 and 90 kcal mol^{-1}, and then, at higher BDE values, it decreases again.[9,10] The KIE_{cal} values are shown in Figure 4b and are seen to reproduce the experimental spike pattern, despite of the fact that some substrates are different vs Figure 4a; what counts is the BDE(C−H) parameter and not the identity of the substrate.

To elucidate the origins of this intriguing pattern, consider Figure 4c,d, which provides KIE_{cal} ($S = 1$) plots vs the corresponding reaction energy (ΔE_R). The ΔE_R quantity is the BDE difference of the bonds that are broken and made in the H-abstraction reactions, ΔE_R = BDE(C−H) − BDE(FeO−H). The computed BDE(FeO−H) values for **1** and **2** are 81.3 and 84.3 kcal mol^{-1}, respectively (Tables S8, S9). As such, both **1** and **2** span a ΔE_R range with the series of hydrocarbons studied here; from exothermic, −14.3 and −16.1 kcal mol^{-1} to endothermic values, + 8.8 and +6.6 kcal mol^{-1}. Hence, ΔE_R divides Figures 4c,d into two zones; the highly exothermic/endothermic zone and the "thermo-neutral" zone, where ΔE_R is around zero. These zones represent the different chemical surroundings of the abstracted H atom; the exothermic zone belongs to conjugated C−H bonds, while the endothermic one to aliphatic C−H.

The ΔE_R quantity is the dominant factor of the tunneling in these reaction series. Thus, in the first zone, the exo/endothermicity of the reaction leaves less of an energy space to tunnel through the barrier. Therefore, in this region the transmission coefficients (Tables S8, S9) and hence also the KIE are diminished (see e.g., the reactions with **CHD**, **DHA** and **DMB**, **CHA**). On the other hand, near the thermo-neutral region the entire energy profile is available for tunneling through the barrier, and hence the transmission coefficients and corresponding KIEs are higher than in the first zone. Additionally, within each zone, the order of transmission coefficients and KIEs is determined by the imaginary frequencies of the corresponding TSs; the larger these frequencies are the narrower the corresponding energy barriers, and the larger are the transmission coefficients and KIE values. For example, for the reaction of **1** in the ΔE_R range from −5.0 to 1.3 kcal mol^{-1}, the imaginary frequencies are 1811−1907 cm^{-1}, and the reaction with the largest frequency has the largest transmission coefficient and highest KIE. Such an imaginary frequency-controlled trend was observed for the C−H activation reactions of $Fe^{IV}O(TMC)(L_{ax})$ complexes with a number of axial ligands (L_{ax})[6] and quasi-constant ΔE_R values. Consequently, the imaginary frequencies dominated tunneling, and the thiolate ligand, $L_{ax} = SCH_2^-$, with the highest imaginary frequency, exhibited the highest amount of tunneling.[6] In the present series, the imaginary frequency effect is dominant only within the zones. It is the reaction energy that dominates the global behavior by varying the portion of the energy barrier available for tunneling. As such, the reaction energy is the parameter responsible for the observed[9,10] and computed spike-like patterns of the KIE plots in Figure 4.

Thus, for the present study, the quantal phenomenon of tunneling does not disrupt the classical BEP rate-equilibrium behavior (Figure 3), and at the same time the reaction energy shapes the KIE pattern (Figure 4). So, despite its quantal origins, the tunneling behavior in Figure 4 resembles the classical Melander−Westheimer pattern for the variation of semi classical KIE with ΔE_R changes during H-abstraction.[17] Similar trends were reported by Koshino et al.[18] for tunneling-containing KIE values in a series of C−H activation reactions of N-oxyl radical with a set of substrates.

As found recently[7] and here too, for all the substrates studied, the calculated free energy barriers, $\Delta G^{\ddagger}_{cal}$, for the $S = 2$ state are smaller than those for the $S = 1$ state, on average by 2.6 and 6.7 kcal mol^{-1}, for **1** and **2**, respectively. Since higher barriers are also narrower barriers with larger imaginary frequencies, then, in line with previous findings[4a,6] the tunneling is much larger here for the $S = 1$ state. Consequently, the corresponding effective free energy barriers, $\Delta G^{\ddagger}_{eff\text{-}cal}$, are lowered by tunneling relative to the $S = 2$ barriers. For **1**, the tunneling correction lowers the average energy difference to 0.66 kcal mol^{-1}, and for four of the substrates it reverses the state ordering, making the $S = 1$ TS lower in energy. For **2**, the tunneling correction lowers to average gap to 4.8 kcal mol^{-1}, but it does not reverse the spin-state ordering in the TS.

Despite the fact that the $S = 2$ TS is still lower in energy, for many of the cases studied here, the computed KIE_{cal} values for $S = 2$ are much too small (~6−14, Tables S3, S4) to match the corresponding KIE_{exp} values, for most cases. On the other hand, the KIE_{cal} values for $S = 1$ are in good match to the KIE_{exp} data. Since KIE_{exp} is a kinetic observable, its value spots the reactive state, and we are led to the conclusion that the downsizing effect of the $S = 1$ barrier by tunneling in conjunction with nonunity spin inversion probabilities[7,13a] combines to make the $S = 1$ state the primary reactive state in **1** and **2**. Still, however, the reactions of **1** + **TL** and **2** + **CHA** proceed by TSR, and most likely small fractions[7] of other reactions, and especially of the deuterated substrates, also proceed via $S = 2$ without changing significantly the KIE. The present reactions of **1** and **2** are different than those studied before[4a,6] for C−H activation reactions of $Fe^{IV}O(TMC)(L_{ax})$ and similar complexes, where the KIE_{exp} values uniformly support $S = 2$ reactivity.

In conclusion, the C−H activation of the nonheme Fe(IV)O complexes, **1** and **2**, exhibits simultaneously a BEP correlation

DOI: 10.1021/jacs.5b12077
J. Am. Chem. Soc. 2016, 138, 2094−2097

and high H/D KIEs, which reveal (Figures 2a, 3a, 4a) also the presence of hydrogen tunneling. Additionally, the plot of the KIE(S = 1) vs the BDE(C−H) of the hydrocarbon exhibits (Figure 4a) a spike-like appearance with the highest KIEs occurring for intermediate values of BDE(C−H), while smaller ones are observed for low and high BDE(C−H) values. Our study shows that the observed KIE_{exp} values serve as probes of the reactive spin state of **1** and **2**. Thus, with the exception of **1** + **TL** and **2** + **CHA** which seem to proceed by crossover from the S = 1 ground state to the S = 2 TS, all other reactions exhibit a good match of the calculated KIE_{cal} (S = 1) values to the experimentally observed KIE_{exp} ones. The spike-like patterns of the KIE vs BDE(C−H) plots were also reproduced by the calculations (KIE_{cal} in Figure 4b−d). Thus, for small and large BDE(C−H) values (e.g., **CHD** and **CHA**), where the reactions are exothermic and endothermic, the molecular system can tunnel through only a fraction of the energy profile and exhibits therefore smaller tunneling and KIE values. For hydrocarbons with intermediate BDE(C−H) values (e.g., **CM**, **EB**), the reactions are nearly thermoneutral, and their energy profiles are entirely accessible for tunneling, thus leading to high tunneling and KIE values. These trends in the reaction energies and hence also in the KIE values reflect the chemical environments of the C−H bonds undergoing activation, which change from conjugated C−H bond to aliphatic ones. As such, the KIEs exhibit Melander−Westheimer patterns, despite the quantal origins of the KIE.[17] In turn, the quasi-constant tunneling correction of the barriers conserves a BEP-like relationship (Figure 3).

Previous interpretations[9] of the spiked-KIE assumed wave-like propagation of the reacting molecular complex from the flat S = 2 surface through the S = 1 barrier for H, in a manner dependent on BDE(C−H) vs a classical over the barrier passage for D. This is still an alternative mechanism, but its verification requires tools entirely different than the ones used herein. In any event, the conclusion that KIE measurements are probes and kinetic signatures[4a] of the reactive spin state is powerful and can be used to guide experimentalists in the ubiquitous TSR.[4a,6,7,15] This underscores the selective role of tunneling, discovered by Schreiner et al.[19]

■ ASSOCIATED CONTENT

Supporting Information

The Supporting Information is available free of charge on the ACS Publications website at DOI: 10.1021/jacs.5b12077.

Computational details and data and full ref 14b (PDF)

■ AUTHOR INFORMATION

Corresponding Author

*sason@yfaat.ch.huji.ac.il

Notes

The authors declare no competing financial interest.

■ ACKNOWLEDGMENTS

S.S. is supported by the Israeli Science Foundation (ISF 1183-13). This paper is dedicated to a teacher, Roald Hoffmann.

■ REFERENCES

(1) (a) Nam, W. *Acc. Chem. Res.* **2007**, *40*, 522. (b) Oloo, W. N.; Que, L. *Acc. Chem. Res.* **2015**, *48*, 2612. (c) Abram, S. L.; Monte-Pérez, I.; Pfaff, F. F.; Farquhar, E. R.; Ray, K. *Chem. Commun.* **2014**, *50*, 9852. (d) Borovik, A. S. *Chem. Soc. Rev.* **2011**, *40*, 1870. (e) Pratt, I.; Mathieson, J. S.; Güell, M.; Ribas, X.; Luis, J. M.; Cronin, L.; Costas, M. *Nat. Chem.* **2011**, *3*, 788. (f) Bigi, M. A.; Reed, S. A.; White, M. C. *Nat. Chem.* **2011**, *3*, 216. (g) Ji, L.; Franke, A.; Brindell, M.; Oszajca, M.; Zahl, A.; van Eldik, R. *Chem. - Eur. J.* **2014**, *20*, 14437.

(2) (a) Schröder, D.; Shaik, S.; Schwarz, H. *Acc. Chem. Res.* **2000**, *33*, 139. (b) Shaik, S.; Danovich, D.; Schröder, D.; Schwarz, H. *Helv. Chim. Acta* **1995**, *78*, 1393.

(3) (a) Bell, R. P. *Proc. R. Soc. London, Ser. A* **1936**, *154*, 414. (b) Evans, M. G.; Polanyi, M. *Trans. Faraday Soc.* **1938**, *34*, 11. (c) Mayer, J. M. *Acc. Chem. Res.* **2011**, *44*, 36.

(4) (a) England, J.; Prakash, J.; Cranswick, M. A.; Mandal, D.; Guo, Y.; Münck, E.; Shaik, S.; Que, L. *Inorg. Chem.* **2015**, *54*, 7828. (b) Schwarz, H. *Isr. J. Chem.* **2014**, *54*, 1413.

(5) (a) Ray, K.; England, J.; Fiedler, A. T.; Martinho, M.; Münck, E.; Que, L. *Angew. Chem., Int. Ed.* **2008**, *47*, 8068. (b) Sastri, C. V.; Lee, J.; Oh, K.; Lee, Y. J.; Lee, J.; Jackson, T. A.; Ray, K.; Hirao, H.; Shin, W.; Halfen, J. A.; Kim, J.; Que, L., Jr.; Shaik, S.; Nam, W. *Proc. Natl. Acad. Sci. U. S. A.* **2007**, *104*, 19181.

(6) Mandal, D.; Ramanan, R.; Usharani, D.; Janardanan, D.; Wang, B.; Shaik, S. *J. Am. Chem. Soc.* **2015**, *137*, 722.

(7) Kwon, Y. H.; Mai, B. K.; Lee, Y.-M.; Dhuri, S. N.; Mandal, D.; Cho, K.-B.; Kim, Y.; Shaik, S.; Nam, W. *J. Phys. Chem. Lett.* **2015**, *6*, 1472.

(8) Kaizer, J.; Klinker, E. J.; Oh, N. Y.; Rohde, J.-U.; Song, W. J.; Stubna, A.; Kim, J.; Münck, E.; Nam, W.; Que, L. *J. Am. Chem. Soc.* **2004**, *126*, 472.

(9) Klinker, E. J.; Shaik, S.; Hirao, H.; Que, L., Jr. *Angew. Chem., Int. Ed.* **2009**, *48*, 1291.

(10) Klinker, E. J. Ph.D. Dissertation. Department of Chemistry, University of Minnesota, Minneapolis, MN.

(11) Truhlar, D. G.; Gao, J.; Alhambra, C.; Garcia-Viloca, M.; Corchado, J.; Sánchez, M. L.; Villà, J. *Acc. Chem. Res.* **2002**, *35*, 341.

(12) (a) Geng, C.; Ye, S.; Neese, F. *Angew. Chem., Int. Ed.* **2010**, *49*, 5717. (b) Kazaryan, A.; Baerends, E. J. *ACS Catal.* **2015**, *5*, 1475. (c) de Visser, S. P. *J. Am. Chem. Soc.* **2006**, *128*, 15809. (d) Wilson, S. A.; Chen, J.; Hong, S.; Lee, Y.-M.; Clémancey, M.; Garcia-Serres, R.; Nomura, T.; Ogura, T.; Latour, J.-M.; Hedman, B.; Hodgson, K. O.; Nam, W.; Solomon, E. I. *J. Am. Chem. Soc.* **2012**, *134*, 11791.

(13) (a) Chen, J.; Cho, K.-B.; Lee, Y.-M.; Kwon, Y. H.; Nam, W. *Chem. Commun.* **2015**, *51*, 13094. (b) Mitra, M.; Nimir, H.; Demeshko, S.; Bhat, S. S.; Malinkin, S. O.; Haukka, M.; Lloret-Fillol, J.; Lisensky, G. C.; Meyer, F.; Shteinman, A. A.; Browne, W. R.; Hrovat, D. A.; Richmond, M. G.; Costas, M.; Nordlander, E. *Inorg. Chem.* **2015**, *54*, 7152.

(14) Quantum mechanical calculations were done with: (a) *Jaguar*, version 8.0; Schrödinger, LLC: New York, 2011. (b) Frisch, M. J.; et al. *Gaussian 09*, revision D.01; Gaussian, Inc.: Wallingford, CT, 2009. (c) Marenich, A. V.; Cramer, C. J.; Truhlar, D. G. *J. Phys. Chem. B* **2009**, *113*, 6378. (d) Grimme, S.; Ehrlich, S.; Goerigk, L. *J. Comput. Chem.* **2011**, *32*, 1456. (e) Duncan, W. T.; Bell, R. L.; Troung, T. N. *J. Comput. Chem.* **1998**, *19*, 1039.

(15) Mai, B. K.; Kim, Y. *Angew. Chem., Int. Ed.* **2015**, *54*, 3946.

(16) (a) Ard, S. G.; Johnson, R. S.; Melko, J. J.; Mrtinze, O., Jr.; Shuman, N. S.; Ushakov, V. G.; Guo, H.; Troe, J.; Viggiano, A. A. *Phys. Chem. Chem. Phys.* **2015**, *17*, 19709. (b) Harvey, J. N.; Poli, R.; Smith, K. *Coord. Chem. Rev.* **2003**, *238−239*, 347.

(17) Melander, L.; Saunders, W. H. Jr. *Reaction Rates of Isotopic Molecules*; Wiley Interscience: New York, 1980; p 29.

(18) Koshino, N.; Cai, Y.; Espenson, J. H. *J. Phys. Chem. A* **2003**, *107*, 4262.

(19) Schreiner, P. R.; Reisenauer, H. P.; Ley, D.; Gerbig, D.; Wu, C.-H.; Allen, W. D. *Science* **2011**, *332*, 1300.

DOI: 10.1021/jacs.5b12077
J. Am. Chem. Soc. 2016, 138, 2094−2097